Variability of Antarctic circumpolar transport and the Southern Annular Mode associated with the Madden-Julian Oscillation

Adrian J. Matthews

Schools of Environmental Sciences and Mathematics, University of East Anglia, Norwich, UK

Michael P. Meredith[1]

Proudman Oceanographic Laboratory, Bidston, Merseyside, UK

[1] The variability of oceanic Antarctic circumpolar transport and the atmospheric Southern Annular Mode (SAM) on intraseasonal (30–70-day) timescales is shown to be related to the tropical atmospheric Madden-Julian Oscillation (MJO) during southern winter. Approximately 7 days after anomalous MJO convection in the equatorial Indian Ocean peaks, an atmospheric extratropical response is set up with anomalous surface westerlies around almost the entire latitude circle at 60°S. This pattern projects strongly onto the SAM and leads to an acceleration of the eastward circumpolar transport around Antarctica, as measured by tide gauges and bottom pressure recorders. This ocean response is confirmed by a global ocean model, which shows a maximum in the transport through Drake Passage 3 days after the atmospheric extratropical response. *INDEX TERMS:* 3374 Meteorology and Atmospheric Dynamics: Tropical meteorology; 4207 Oceanography: General: Arctic and Antarctic oceanography; 1620 Global Change: Climate dynamics (3309); 3339 Meteorology and Atmospheric Dynamics: Ocean/atmosphere interactions (0312, 4504); 4556 Oceanography: Physical: Sea level variations. **Citation:** Matthews, A. J., and M. P. Meredith (2004), Variability of Antarctic circumpolar transport and the Southern Annular Mode associated with the Madden-Julian Oscillation, *Geophys. Res. Lett.*, *31*, L24312, doi:10.1029/2004GL021666.

1. Introduction

[2] Analysis of tide gauge and bottom pressure recorder (BPR) data has shown that oceanic subsurface pressure (SSP; sea level corrected for the "inverse barometer effect") and bottom pressure vary coherently around Antarctica on timescales from intraseasonal to interannual, coincident with changes in the oceanic circumpolar transport [*Aoki*, 2002; *Hughes et al.*, 2003; *Meredith et al.*, 2004]. Surface westerly (easterly) wind anomalies around the Southern Ocean close to Antarctica accelerate (decelerate) the oceanic circumpolar transport, associated with a fall (rise) in SSP and bottom pressure at the edge of the continent itself. These transport changes are predominantly barotropic at subseasonal timescales, and are strongly steered by potential vorticity contours that almost circumnavigate Antarctica [*Hughes et al.*, 1999].

[3] The surface wind anomalies that force this oceanic mode project strongly onto the Southern Annular Mode (SAM), the primary atmospheric mode of variability in the Southern Hemisphere [*Rogers and van Loon*, 1982; *Thompson and Wallace*, 2000]. The SAM comprises an approximately zonally symmetric sea-saw in pressure between high latitudes and the subtropics, with associated geostrophically balanced zonal wind anomalies centred approximately along 60°S.
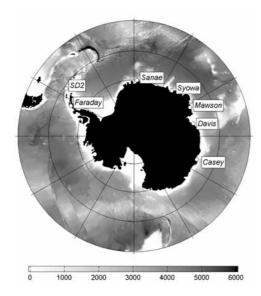
[4] Tropical variability on interannual timescales (ENSO) has been shown to affect Antarctica [*Turner*, 2004]. Here we examine tropical-Antarctic variability on intraseasonal timescales. The dominant mode of intraseasonal variability in the tropical atmosphere is the Madden-Julian Oscillation (MJO) [*Madden and Julian*, 1994], where large-scale (10,000 km across) convective anomalies propagate slowly eastward from the Indian Ocean to the western Pacific with a period of approximately 30–70 days. Tropical pressure, temperature and wind anomalies develop as a moist equatorial Kelvin-Rossby wave response to the convective anomalies [*Hendon and Salby*, 1994]. There is also an extratropical component of the MJO which tends to be strongest in the winter hemisphere [*Kiladis and Mo*, 1998]. During the northern winter at least, this can be simulated as a response to the tropical convective anomalies [*Matthews et al.*, 2004].

[5] This extratropical component will include surface wind anomalies in the high southern latitudes that could potentially force the oceanic circumpolar mode. In this paper, we look for such a relationship between the MJO and Antarctic circumpolar transport.

2. Data

[6] The BPR and tide gauge pressure data used are described in detail by *Hughes et al.* [2003]. The stations cover approximately half of the Antarctic coast, from Faraday on the Antarctic Peninsula at 65°W to Casey at 110°E (Figure 1). The data were detided, with daily means then derived and gaps filled by interpolation. Individual BPR time series are typically of one year in duration; these were concatenated via endpoint matching. Although periods longer than the duration of single BPR deployments are not well-represented in these data, signals with the timescales under study here are reliably depicted. A time series of transport through Drake Passage was taken from the 0.25° OCCAM global ocean model, forced by 6-hourly ECMWF reanalysis winds [*Webb and de Cuevas*, 2002].

[7] A daily SAM index calculated from the NOAA Climate Data Assimilation System reanalysis was used, as

---

[1]Now at British Antarctic Survey, Cambridge, UK.

Figure 1. Locations of the tide gauge and bottom pressure recorder stations. Ocean depth (m) is shaded. See color version of this figure in the HTML.

by *Hughes et al.* [2003]. Atmospheric wind data were taken from the NCEP-NCAR reanalysis and satellite-measured outgoing longwave radiation (OLR) data were used as a proxy for tropical convection. All data were passed through a 30–70-day band-pass Lanczos filter with 241 daily weights to isolate the intraseasonal variability. The results presented here are only for southern winter (May–October), as this is the season when the relationship between the MJO and the high southern latitudes is expected to be strongest. The calculations were repeated for the southern summer season and for year-round data, but no significant results were found for these cases.

3. Results

3.1. Antarctic Stations

[8] It has been demonstrated that the BPR at the south side of Drake Passage (SD2; Figure 1) yields a reliable index of the oceanic transport through Drake Passage [*Meredith et al.*, 1996, 2004]; it has the added benefit of providing an almost continuous record, such that the 30–70-day filtered time series runs from 24 March 1990 to 29

July 2000. The intraseasonal fluctuations in the bottom pressure at SD2 are highly correlated (statistically significant at the 95% level) and vary almost simultaneously with those at the other Antarctic stations, from Faraday round to Casey (Table 1) [*Hughes et al.*, 2003]. For example, the maximum lagged correlation between SD2 and Faraday is a statistically significant $r = 0.77$, with Faraday peaking 1 day before SD2.

[9] The intraseasonal fluctuations in pressure at SD2, and therefore at all the other Antarctic stations, are also simultaneously anti-correlated with the eastward transport through Drake Passage, as calculated by the OCCAM model ($r = -0.70$ at a lag of 1 day; Table 1). Hence, the SD2 time series is a reasonable proxy for oceanic circumpolar transport. This echoes the results of *Hughes et al.* [2003], who demonstrated coherence around Antarctica on a broader range of timescales.

3.2. Surface Wind Anomalies

[10] The 30–70-day filtered surface winds from the reanalysis were regressed against the SD2 time series for southern winter (see *Kiladis and Weickmann* [1992] for regression technique). When scaled for a −2 standard deviation in the SD2 time series, i.e., a strong negative anomaly in subsurface pressure off the Antarctic coast, the regression map shows a band of surface westerly anomalies around the entire latitude belt between 55° and 65°S (Figures 2a and 3), consistent with the circumpolar transport forcing arguments described above. This wind pattern will project onto the SAM. The SD2 and SAM indices are almost simultaneously anti-correlated on intraseasonal timescales, with a minimum correlation coefficient of $r = -0.66$ when the SAM leads SD2 by 2 days (Table 1). The surface wind anomalies regressed onto the SAM index and lagged by 2 days, to coincide with the minimum in SD2 bottom pressure, are shown in Figure 2b. The westerly anomalies along 60°S can be clearly seen.
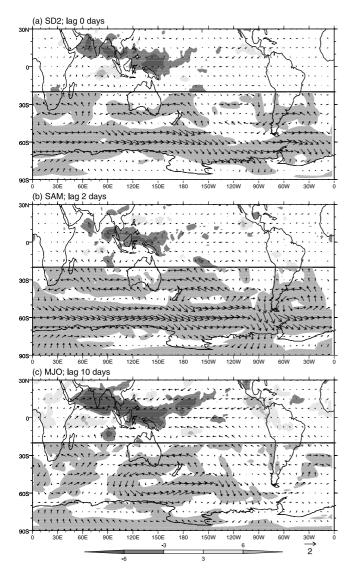
3.3. Madden-Julian Oscillation

[11] The bottom pressure variations at SD2 are also coherently related to intraseasonal fluctuations in tropical convection, such that when the SD2 pressure is low there is a band of enhanced convective rainfall (negative OLR anomalies) from the northern Indian Ocean, through southeast Asia, to the equatorial western Pacific (Figure 2a). This

Table 1. Maximum/Minimum Lagged Correlations Between 30–70-Day Filtered Time Series (First Column; See Figure 1 for Station Codes) and the SD2 (Second Column) and MJO (Third Column) Time Series, for Southern Winter[a]

Time series	SD2	MJO (PC 1)	Time domain	r_c
Faraday	**0.77** (−1)	**−0.35** (8)	1990–99	0.15
SD2	**1.00** (0)	**−0.39** (11)	1990–99	0.15
Sanae	**0.92** (0)	**−0.41** (9)	1993–95	0.28
Syowa	**0.78** (0)	**−0.59** (10)	1994–99	0.19
Mawson	**0.75** (−1)	**−0.36** (10)	1993–99	0.17
Davis	**0.75** (−1)	**−0.32** (9)	1994–98	0.21
Casey	**0.79** (−2)	−0.24 (9)	1997–98	0.34
Transport	**−0.70** (1)	**0.19** (12)	1993–97	0.18
SAM	**−0.66** (−2)	**0.32** (7)	1990–99	0.15
MJO (PC 2)	**−0.34** (0)	**0.61** (10)	1990–99	0.15

[a]Statistically significant values are shown in bold. The lag at which the maximum/minimum correlation occurs is shown in brackets; a positive (negative) lag means the relevant time series lags (leads) the SD2/MJO time series. The fourth column shows the May–October seasons over which the correlations were calculated. The critical correlation coefficient r_c which must be exceeded for statistical significance at the 95% level is in the fifth column.

Figure 2. Southern winter regression maps of 30−70-day filtered surface vector wind and OLR, regressed against various indices and lagged to coincide with minimum bottom pressure at SD2. (a) Zero lag, regressed against SD2 and scaled for −2 standard deviations. (b) 2-day lag, regressed against SAM and scaled for 2 standard deviations. (c) 10-day lag, regressed against the MJO index and scaled for 2 standard deviations. The reference wind vector is 2 m s^{-1}. OLR anomalies are shaded red and blue (see legend) from 20°S to 30°N. Yellow shading between 90°S and 20°S shows where either the u or v component of the wind anomalies is locally significant at the 95% level. See color version of this figure in the HTML.
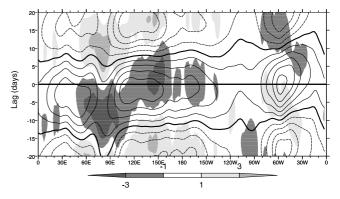
convection pattern corresponds to one phase of the MJO during southern winter [*Annamalai and Slingo*, 2001]. A time (lag)−longitude diagram of tropical OLR anomalies regressed against SD2 (Figure 3) shows the eastward propagation of the OLR anomalies, confirming the relationship with the MJO.

[12] Further confirmation is gained by an empirical orthogonal function (EOF) analysis of filtered OLR over the tropical warm pool region (a standard technique for
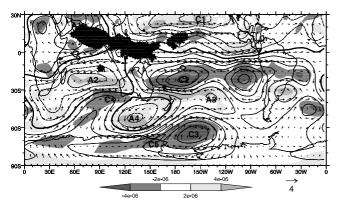
identifying the MJO; for details see *Matthews* [2000]). Such an EOF analysis for the May−October season produces two leading eigenvectors (EOFs) which are spatially and temporally in quadrature, and together describe the eastward and northward propagating convective anomalies that comprise the MJO during southern winter. A principal component (PC) time series can be calculated by projecting the EOF spatial structure onto the daily maps of anomalous OLR. The PC 2 time series has a maximum lagged correlation with PC 1 of 0.61 when it lags by 10 days (Table 1). This reflects the typical 40-day period of the MJO. From here, we will just use PC 1 as our MJO index; similar results were obtained from PC 2, but with a 10 day lag.

[13] The SD2 time series has a minimum correlation with the PC 1 MJO index of $r = -0.39$ at a lag of 11 days (Table 1). Hence, up to 15% of the intraseasonal variance in SD2 can be accounted for by linear variations in the MJO index. Time series from all the other stations have minimum correlations at lags of 8−10 days after the MJO index. All are significant at the 95% level, except Casey. The correlation between the MJO and the transport through Drake Passage from the OCCAM model reaches a maximum a few days later, at a lag of 12 days. Although just significant, the magnitude of the correlation ($r = 0.19$) is rather small, reflecting the complex chain of physical processes by which the MJO leads to circumpolar transport changes in this model.

[14] We can now construct regression maps based on the MJO itself, using PC 1 as the reference time series. The regression map of anomalous OLR and surface wind, lagged by 10 days with respect to the MJO index (Figure 2c), is similar to the (near) simultaneous regression maps based on SD2 (Figure 2a) and the SAM (Figure 2b), with enhanced convection from the northern Indian Ocean to the equatorial western Pacific (maximum correlations locally reach 0.5) and surface westerly anomalies around almost the entire latitude belt at 60°S, although there are much stronger zonal asymmetries here. Hence, it appears that the high-latitude wind forcing that drives the intra-

Figure 3. Hovmöller diagram of anomalous OLR averaged over 20°S−20°N, and surface zonal wind anomalies at 60°S regressed against the SD2 (scaled for −2 standard deviations). OLR anomalies are shaded (see legend). Zonal wind contour interval is 0.5 m s^{-1}; negative contours are dashed, and the zero contour is thickened. See color version of this figure in the HTML.

Figure 4. Regression map of 30–70-day filtered OLR and 200-hPa vorticity, vector wind and stream function, regressed against the MJO index and lagged by 10 days: OLR anomalies are grey shaded darkly below -6 W m^{-2} and lightly above 6 W m^{-2}. Negative vorticity anomalies are shaded blue and positive vorticity anomalies are shaded red (see legend). The reference wind vector is 4 m s^{-1}. Stream function contour interval is 1×10^6 m^2 s^{-1}; negative contours are dashed. Selected anticyclonic and cyclonic anomalies are indicated by "A" and "C", respectively. See color version of this figure in the HTML.

seasonal fluctuations in bottom pressure and transport through Drake Passage are themselves related to the MJO.

3.4. Tropical-Extratropical Interaction

[15] The mechanism by which the tropical convective anomalies lead to high-latitude surface wind anomalies is explored briefly here. The 10-day lagged map of OLR with respect to the MJO index (Figure 4) shows a region of enhanced convection (negative OLR anomalies, shaded in dark grey) from India to the equatorial western Pacific, as in Figure 2c. The anomalous tropical anticyclones (A1, A2), cyclones (C1, C2) and equatorial easterlies over the Pacific can be interpreted as an equatorial Rossby-Kelvin wave response to the anomalous tropical heating [*Hendon and Salby*, 1994]. Extratropical Rossby wave trains emanate from these tropical anomalies in the Pacific (C2, A3, C3) and Indian (A2, C4, A4, C5) sectors; their development can be traced at earlier lags (not shown). These anomalies are similar to those by *Kiladis and Mo* [1998] and *Revell et al.* [2001], and have a similar scale to the Pacific–South American modes of extratropical variability [*Mo and Higgins*, 1998] that are also related to MJO convection, but do not appear to project strongly onto them. The tropical anomalies have a baroclinic structure with opposite sign between the upper and lower troposphere, consistent with the Gill model of tropical heating [*Hendon and Salby*, 1994]. The extratropical anomalies have an equivalent barotropic structure and extend from the upper troposphere down to the surface, where the surface westerly wind anomalies along 60°S in Figure 2c over the Pacific sector are related to the A4, C5 and C3 vorticity anomalies in Figure 4. Other processes may also play a part in the extratropical response to the MJO: e.g., wave–mean flow interaction and barotropic and baroclinic instability [*Kiladis and Mo*, 1998], and propagation of an atmospheric Kelvin

wave eastward along the equator over the Pacific, then southward as a trapped wave against the Andes [*Matthews*, 2000]. The dynamics alluded to here are complex, and there is scope for more study to elucidate them further.

4. Conclusions

[16] Intraseasonal fluctuations in oceanic subsurface pressure and zonal transport around at least half of Antarctica vary coherently and are related to changes in MJO tropical convection during southern winter, such that seven days after MJO convection peaks in the equatorial Indian Ocean, the SAM reaches a maximum, followed by a maximum in the circumpolar transport three days later. The tropical part of the MJO can be predicted skillfully up to 20 days ahead [e.g., *Wheeler and Weickmann*, 2001] and the skill of extratropical forecasts improves when the tropical MJO is well represented in an NWP model [*Ferranti et al.*, 1990]. Given that up to 15% of the intraseasonal variance in the oceanographic data can be linearly accounted for by the MJO, then efforts to forecast fluctuations in Antarctic circumpolar transport thus need to consider intraseasonal forcings from the tropics as well as high latitudes; the lag between tropical forcing and transport response may assist such efforts. The MJO affects land surface temperatures in high northern latitudes [*Vecchi and Bond*, 2004], and an analysis of the relationship between the MJO and Antarctic land surface temperatures is underway.

References

Annamalai, H., and J. M. Slingo (2001), Active/break cycles: Diagnosis of the intraseasonal variability of the Asian summer monsoon, *Clim. Dyn.*, *18*, 85–102.

Aoki, S. (2002), Coherent sea level response to the Antarctic Oscillation, *Geophys. Res. Lett.*, *29*(20), 1950, doi:10.1029/2002GL015733.

Ferranti, L., et al. (1990), Tropical-extratropical interaction associated with the 30–60 day oscillation and its impact on medium and extended range prediction, *J. Atmos. Sci.*, *47*, 2177–2199.

Hendon, H. H., and M. L. Salby (1994), The life cycle of the Madden-Julian Oscillation, *J. Atmos. Sci.*, *51*, 2225–2237.

Hughes, C. W., et al. (1999), Wind-driven transport fluctuations through Drake Passage: A southern mode, *J. Phys. Oceanogr.*, *29*, 1971–1992.

Hughes, C. W., et al. (2003), Coherence of Antarctic sea levels, Southern Hemisphere Annular Mode, and flow through Drake Passage, *Geophys. Res. Lett.*, *30*(9), 1464, doi:10.1029/2003GL017240.

Kiladis, G. N., and K. C. Mo (1998), Interannual and intraseasonal variability in the Southern Hemisphere, in *Southern Hemisphere Meteorology*, edited by D. J. Karoly and D. G. Vincent, pp. 307–336, Am. Meteorol. Soc., Washington, D. C.

Kiladis, G. N., and K. M. Weickmann (1992), Circulation anomalies associated with tropical convection during northern winter, *Mon. Weather Rev.*, *120*, 1900–1923.

Madden, R. A., and P. R. Julian (1994), Observations of the 40–50 day tropical oscillation—A review, *Mon. Weather Rev.*, *122*, 814–837.

Matthews, A. J. (2000), Propagation mechanisms for the Madden-Julian Oscillation, *Q. J. R. Meteorol. Soc.*, *126*, 2637–2652.

Matthews, A. J., et al. (2004), The global response to tropical heating in the Madden-Julian Oscillation during northern winter, *Q. J. R. Meteorol. Soc.*, *130*, 1991–2011.

Meredith, M. P., et al. (1996), On the temporal variability of the transport through Drake Passage, *J. Geophys. Res.*, *101*, 22,485–22,494.

Meredith, M. P., et al. (2004), Changes in the ocean transport through Drake Passage during the 1980s and 1990s, forced by changes in the Southern

Annular Mode, *Geophys. Res. Lett.*, *31*(21), L21305, doi:10.1029/2004GL021169.

Mo, K. C., and R. W. Higgins (1998), The Pacific-South American modes and tropical convection during the Southern Hemisphere winter, *Mon. Weather Rev.*, *126*, 1581–1596.

Revell, M. J., et al. (2001), Interpreting low-frequency modes of Southern Hemisphere atmospheric variability as the rotational response to divergent forcing, *Mon. Weather Rev.*, *129*, 2416–2425.

Rogers, J. C., and H. van Loon (1982), Spatial variability of sea-level pressure and 500 mb height anomalies over the Southern Hemisphere, *Mon. Weather Rev.*, *110*, 1375–1392.

Thompson, D. W. J., and J. M. Wallace (2000), Annular modes in the extratropical circulation. Part I: Month-to-month variability, *J. Clim.*, *13*, 1000–1016.

Turner, J. (2004), The El Niño–Southern Oscillation and Antarctica, *Int. J. Climatol.*, *24*, 1–31.

Vecchi, G. A., and N. A. Bond (2004), The Madden-Julian Oscillation (MJO) and northern high latitude wintertime surface air temperatures, *Geophys. Res. Lett.*, *31*, L04104, doi:10.1029/2003GL018645.

Webb, D. J., and B. A. de Cuevas (2002), An ocean resonance in the southeast Pacific, *Geophys. Res. Lett.*, *29*(8), 1252, doi:10.1029/2001GL014259.

Wheeler, M., and K. M. Weickmann (2001), Real-time monitoring and prediction of modes of coherent synoptic to intraseasonal tropical variability, *Mon. Weather Rev.*, *129*, 2677–2694.

———————————

A. J. Matthews, School of Environmental Sciences, University of East Anglia, Norwich NR4 7TJ, UK. (a.j.matthews@uea.ac.uk; internet: http://envam1.env.uea.ac.uk)

M. P. Meredith, British Antarctic Survey, High Cross, Madingley Road, Cambridge CB3 0ET, UK.